In Vitro Targeted Photodynamic Therapy With a Pyropheophorbide-a Conjugated Inhibitor of Prostate-Specific Membrane Antigen

Tiancheng Liu, Lisa Y. Wu, Joseph K. Choi, and Clifford E. Berkman*

Department of Chemistry, Washington State University, Pullman, Washington

BACKGROUND. The lack of specific delivery of photosensitizers (PSs), represents a significant limitation of photodynamic therapy (PDT) of cancer. The biomarker prostate-specific membrane antigen (PSMA) has attracted considerable attention as a target for imaging and therapeutic applications for prostate cancer. Although recent efforts have been made to conjugate inhibitors of PSMA with imaging agents, there have been no reports on PS-conjugated PSMA inhibitors for targeted PDT of prostate cancer. The present study focuses on the use of a PSMA inhibitor-conjugate of pyropheophorbide-a (Ppa-conjugate **2**) for targeted PDT to achieve apoptosis in PSMA+ LNCaP cells.

METHODS. Confocal laser scanning microscopy with a combination of nuclear staining and immunofluorescence methods were employed to monitor the specific imaging and PDT-mediated apoptotic effects on PSMA-positive LNCaP and PSMA-negative (PC-3) cells.

RESULTS. Our results demonstrated that PDT-mediated effects by Ppa-conjugate **2** were specific to LNCaP cells, but not PC-3 cells. Cell permeability was detected as early as 2 hr by HOE33342/PI double staining, becoming more intense by 4 hr. Evidence for the apoptotic caspase cascade being activated was based on the appearance of poly-ADP-ribose polymerase (PARP) p85 fragment. Terminal deoxynucleotidyl transferase dUTP nick end labeling (TUNEL) assay detected DNA fragmentation 16 hr post-PDT, confirming apoptotic events.

CONCLUSIONS. Cell permeability by HOE33342/PI double staining as well as PARP p85 fragment and TUNEL assays confirm cellular apoptosis in PSMA+ cells when treated with PS-inhibitor conjugate **2** and subsequently irradiated. It is expected that the PSMA targeting small-molecule of this conjugate can serve as a delivery vehicle for PDT and other therapeutic applications for prostate cancer. *Prostate 69: 585–594, 2009.*

KEY WORDS: **PSMA; targeted photodynamic therapy; pyropheophorbide-a; prostate cancer; apoptosis**

INTRODUCTION

Photodynamic therapy (PDT) has emerged as a non-invasive regimen for cancer treatment thus representing an attractive alternative to conventional therapies [1–8]. Furthermore, PDT can be employed for both therapeutic and imaging purposes when the photosensitizer (PS) fluoresces in the near-IR range [9]. Despite its promise, PDT is not yet an integral part of clinical cancer therapy practice due to limitations associated with selective tumor targeting [10]. While early-phase clinical trials for prostate cancer indicate that PDT shows potential as a safe treatment option for localized, recurrent disease [10], there remains a need to enhance the targeting capabilities of PSs.

In light of this need, we have focused on developing a method for the targeted delivery of PSs for the selective abrogation of prostate cancer cells. Specifically, we have designed chemical agents that exhibit

Additional Supporting Information may be found in the online version of this article.

Grant sponsor: National Institutes of Health; Grant number: 7R21CA122126-03.

*Correspondence to: Clifford E. Berkman, Department of Chemistry, Washington State University, Pullman, WA 99164-4630.
E-mail: cberkman@wsu.edu

Received 23 October 2008; Accepted 25 November 2008
DOI 10.1002/pros.20909
Published online 13 January 2009 in Wiley InterScience (www.interscience.wiley.com).

high affinity and specificity for the prostate cancer biomarker, prostate-specific membrane antigen (PSMA). PSMA is a type II glycoprotein commonly found on the surface of tumor cells of late stage, androgen-independent, and metastatic prostate cancer [11]. In prostate cancer cells, PSMA is expressed at 1,000-fold higher levels than in normal prostate epithelium [12]. Expression levels increase with disease progression, being highest in metastatic disease, hormone refractory cancers, and higher-grade lesions [12]. Endothelial-expression of PSMA in the neovasculature of a variety of non-prostatic solid malignancies has also been detected [13,14]. Therefore, it is not surprising that PSMA has attracted significant attention as a biomarker and target for the delivery of imaging [15–30] and therapeutic agents [31–34].

We previously reported that phosphoramidate peptidomimetic PSMA inhibitors were capable of both cell-surface labeling of prostate cancer cells and intracellular delivery [35]. In this current study, we describe the conjugation of a peptidomimetic inhibitor of PSMA to the porphyrinic PS, pyropheophorbide-a (Ppa; Fig. 1). Pyropheophorbide-a has been shown to be a potent PS in PDT experiments but alone, it lacks the specificity to effectively target cancer cells [36–38]. In addition, we reveal the capability of Ppa-conjugate **2** to selectively induce apoptosis of prostate cancer cells in vitro. Cellular effects related to apoptosis after PDT were determined by nuclear staining, poly-ADP-ribose polymerase (PARP) p85 fragment immunofluorescence, and the terminal deoxynucleotidyl transferase dUTP nick end labeling (TUNEL) assay, as detected by fluorescence imaging using confocal laser scanning microscopy.

MATERIALS AND METHODS

Cell Lines, Reagents, and General Procedures

LNCaP and PC-3 cells were obtained from the American Type Culture Collection (Manassas, VA). The rabbit polyclonal anti-PARP p85 antibody and goat anti-rabbit IgG-FITC were obtained from Sigma–Aldrich (St. Louis, MO). Normal goat serum was obtained from BioGenex (San Ramon, CA). 4′,6-Diamidino-2-phenylindol dihydrochloride (DAPI) and Hoechst 33342 (HOE33342) were obtained from Invitrogen-Molecular Probes. Propidium iodide (PI) was obtained from MP Biomedicals, LLC (Solon, OH). DeadEnd Fluorometric TUNEL System was obtained from Promega (Madison, WI). Ppa was obtained from Frontier Scientific, Inc. (Logan, UT). All other chemicals and cell-culture reagents were purchased from Fisher Scientific (Sommerville, NJ), Pierce (Rockford, IL), or Sigma–Aldrich. All solvents used in chemical reactions were anhydrous and obtained as such from commercial sources. All other reagents were used as supplied unless otherwise stated. ^{1}H, ^{13}C, and ^{31}P NMR spectra were recorded on a Bruker DRX 300 MHz NMR Spectrometer. ^{1}H NMR chemical shifts are relative to TMS ($\delta = 0.00$ ppm), $CDCl_3$ ($\delta = 7.26$ ppm). ^{13}C NMR chemical shifts are relative to $CDCl_3$ ($\delta = 77.23$ ppm). ^{31}P NMR chemical shifts in $CDCl_3$ was externally referenced to 85% H_3PO_4 ($\delta = 0.00$ ppm) in $CDCl_3$.

Preparation of Ppa-Conjugate 2

The NHS ester of Ppa (Ppa-NHS) was prepared as previously described [36]. A solution of Ppa-NHS ester (6 μmol) in 100 μl DMSO was added to a stirred solution of the inhibitor core **1** (2 μmol, 100 μl of 20 mM in H_2O), 160 μl H_2O, and 40 μl of 1 M $NaHCO_3$. The reaction mixture was stirred for 6 hr in the dark at room temperature. The pH of the resulting solution was then adjusted to 9.3 by the addition of 8 μl of 1 M Na_2CO_3. The unreacted inhibitor core **1** was scavenged by stirring with 25 mg of Si–Isocyanate resin (SiliCycle, Inc., Quebec, Canada) overnight at room temperature. The solution was subsequently centrifuged (9,000 rpm, 10 min) and the supernatant was lyophilized in a 2 ml microcentrifuge tube. Unreacted and/or hydrolyzed Ppa-NHS was removed by successively triturating the lyophilized solid with 1 ml portions of DMSO and centrifuging the mixture (1 min at 13,000 rpm) after each wash; this process was repeated 10 times. The Ppa-conjugated inhibitor **2** was dissolved in 50 mM Tris buffer (pH 7.5) to give a final concentration of 2 mM (approximately 800 μl).

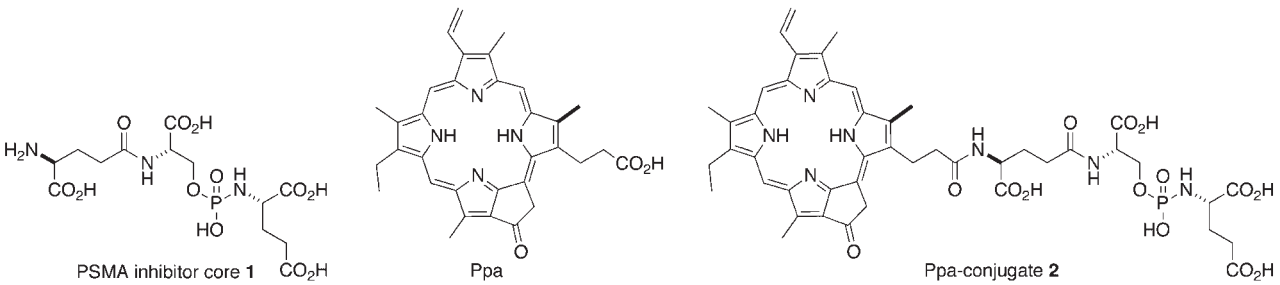

Fig. 1. Structures of phosphoramidate peptidomimetic inhibitor core **1**, Ppa, and its Ppa-conjugate **2**.

IC_{50} Determination for Ppa-Conjugate 2

Inhibition studies were performed as described previously with only minor modifications [35,39]. Working solutions of the substrate (*N*-[4-(phenylazo)-benzoyl]-glutamyl-γ-glutamic acid, PABGgG) and inhibitor were made in TRIS buffer (50 mM, pH 7.4). Working solutions of purified PSMA were diluted in TRIS buffer (50 mM, pH 7.4 containing 1% Triton X–100) to provide from 15% to 20% conversion of substrate to product in the absence of inhibitor. A typical incubation mixture (final volume 250 μl) was prepared by the addition of either 25 μl of an inhibitor solution or 25 μl TRIS buffer (50 mM, pH 7.4) to 175 μl TRIS buffer (50 mM, pH 7.4) in a test tube. PABGgG (25 μl, 10 μM) was added to the above solution. The enzymatic reaction was initiated by the addition of 25 μl of the PSMA working solution. In all cases, the final concentration of PABGgG was 1 μM while the enzyme was incubated with five serially diluted inhibitor concentrations providing a range of inhibition from 10% to 90%. The reaction was allowed to proceed for 15 min with constant shaking at 37°C and was terminated by the addition of 25 μl methanolic TFA (2% trifluoroacetic acid by volume in methanol) followed by vortexing. The quenched incubation mixture was quickly buffered by the addition of 25 μl K_2HPO_4 (0.1 M), vortexed, and centrifuged (10 min at 7,000g). An 85 μl aliquot of the resulting supernatant was subsequently quantified by HPLC as previously described [40,41]. IC_{50} values were calculated using KaleidaGraph 3.6 (Synergy Software).

In Vitro Photodynamic Therapy Experiments

PSMA-positive (PSMA+) cells (LNCaP) and PSMA-negative (PSMA−) cells (PC-3) were grown in T-75 flasks with complete growth medium [RPMI 1640 containing 10% heat-inactivated fetal calf serum (FBS), 100 U of penicillin and 100 μg/ml streptomycin] in a humidified incubator at 37°C and 5% CO_2. Confluent cells were detached with a 0.25% trypsin 0.53 mM EDTA solution, harvested, and plated in two-well slide chambers at a density of 4×10^4 cells/well. Cells were grown for 3–4 days before conducting the following experiments.

In vitro PDT with Ppa-conjugate 2. LNCaP and PC-3 cells grown in two-well slide chambers for 3 days were washed twice in 37°C pre-warmed medium A (phosphate-free RPMI 1640 containing 1% FBS), and then incubated with 1 ml of Ppa-conjugate **2** (2.5 or 5 μM) in pre-warmed medium A for 2.5 hr in a humidified incubator at 37°C and 5% CO_2, which allowed internalization of Ppa-conjugate **2** bound to PSMA to occur. In a competitive challenge experiment, cells were pre-incubated with 100 μM inhibitor core **1** for 30 min prior to incubation with Ppa-conjugate **2** under the same condition described above. Cells treated with Ppa-conjugate **2** were washed in the 37°C pre-warmed phenol-free medium RPMI 1640 once, and then irradiated with white light (7.5 J/cm^2, with 25 mW/cm^2 fluence rate) for 10 min in pre-warmed phenol red-free RPMI 1640. The light source was a 100-W halogen lamp, which was filtered through both a 10 cm column of water and filtered a Lee Primary Red filter (no. 106, Vincent Lighting, Cleveland, OH) to remove light with wavelengths below 600 nm.

TUNEL staining in situ. PDT-treated cells were placed in pre-warmed normal growth medium (normal RPMI 1640 containing 10% FBS and 1% penicillin–streptomycin), and returned to a humidified incubator at 37°C and 5% CO_2 for 16 hr and allowed to recover. The cells were then rinsed twice in ice-cold phosphate-buffered saline (PBS) and fixed with 4% paraformaldehyde in PBS for 15 min at room temperature. The fixed cells were washed twice in cold PBS, permeabilized in 0.2% Triton X–100 solution in PBS for 5 min at room temperature, and rinsed twice in PBS for 5 min at room temperature. The TUNEL assay was performed according to manufacturer's instruction. All treated cells were counterstained with DAPI and mounted in VECTASHIELD® Mounting Medium (Vector Laboratories, Burlingame, CA) for microscopy.

HOE33342/PI double-staining nuclei. Following PDT treatment with Ppa-conjugate **2** at 2.5 μM, cells were incubated with pre-warmed normal growth medium (standard medium RPMI 1640 containing 10% FBS, 1% penicillin–streptomycin), and allowed to recover for 2 and 4 hr in a humidified incubator at 37°C and 5% CO_2. Cells were then rinsed twice with 1 ml of pre-warmed phosphate-free medium RPMI 1640, and then incubated with both 1 ml of phosphate-free medium containing 1 μl of 5 mg/ml HOE33342 (dissolved in H_2O), and 1 μl of 1 mg/ml of PI (dissolved in H_2O) at room temperature for 15 min in the dark. Subsequently, cells were washed twice in ice-cold phosphate-free medium RPMI 1640 and once in ice-cold KRB buffer pH 7.4 (mmol/L: NaCl 154.0, KCl 5.0, $CaCl_2$ 2.0, $MgCl_2$ 1.0, HEPES 5.0, D-glucose 5.0). Lastly, these cells were fixed with freshly prepared 4% paraformaldehyde in KRB for 15 min at room temperature and mounted with VECTASHIELD® Mounting Medium for microscopy.

Detection of PARP p85 fragment. Following PDT treatment, cells were incubated with pre-warmed

normal growth medium (standard RPMI 1640 containing 10% FBS, 1% penicillin–streptomycin), and allowed to recover for 2 and 4 hr in a humidified incubator at 37°C and 5% CO_2. Cells were fixed and permeabilized as described in the above protocol for the Detection of PARP p85 fragment Section. Cells were then blocked for 2 hr in blocking buffer (0.1% Tween-20 with 5% goat normal serum in PBS) at room temperature, rinsed once in PBS, incubated with the anti-PARP p85 fragment antibody (1:100) in blocking buffer at 4°C overnight, then successively washed twice in PBS, 0.1% Tween-20 in PBS, and finally in PBS for 10 min at room temperature. Finally, cells were incubated with the fluorescein conjugate of goat anti-rabbit antibody (1:40) in 1% BSA in PBS for 2 hr at room temperature, counterstained with DAPI, and then mounted in VECTASHIELD® Mounting Medium for microscopy (according to manufacturer's protocol; Invitrogen).

Confocal laser scanning microscopy. Cells were visualized under a 40X oil immersion objective using an LSM 510 META Laser Scanning Microscope with a Diode Laser (405 nm) for DAPI or HOE33342, Ar Laser (488 nm) for Fluorescein, and a HeNe Laser (543 nm) for PI. The pictures were edited by National Institutes of Health (NIH) Image J software (http://rsb.info.nih.gov/ij) and Adobe Photoshop CS2.

RESULTS

Preparation and IC_{50} Evaluation of Ppa-Conjugate 2

Ppa-conjugate **2** was prepared from **1** and Ppa-NHS using coupling conditions described previously for the conjugation of **1** with 5-FAM-X SE [35]. IC_{50} values were determined for both the inhibitor core **1** and the Ppa-conjugate **2** and revealed that both compounds were potent inhibitors of PSMA using an HPLC-based assay previously developed by our group [35,39–41]. The IC_{50} values for inhibitor core **1** and Ppa-conjugate **2** for PSMA purified from LNCaP cells [42] were 14 [35] and 102 nM, respectively.

PDT-Mediated Effects by Ppa-Conjugate 2

Specificity of PDT and Detection of Apoptotic Cells—TUNEL Assay. DNA fragmentation following PDT-treatment with Ppa-conjugate **2** was detected using the TUNEL assay (Fig. 2) [43–47]. Detection of DNA fragmentation using this assay was observed as green fluorescent signals from cell nuclei as a result of incorporation of fluorescein-dUTP. For these experiments, concentrations of 1, 2.5, and 5 μM of Ppa-conjugate **2** were applied to both LNCaP and PC-3 cells prior to light administration. The PDT-treatment of

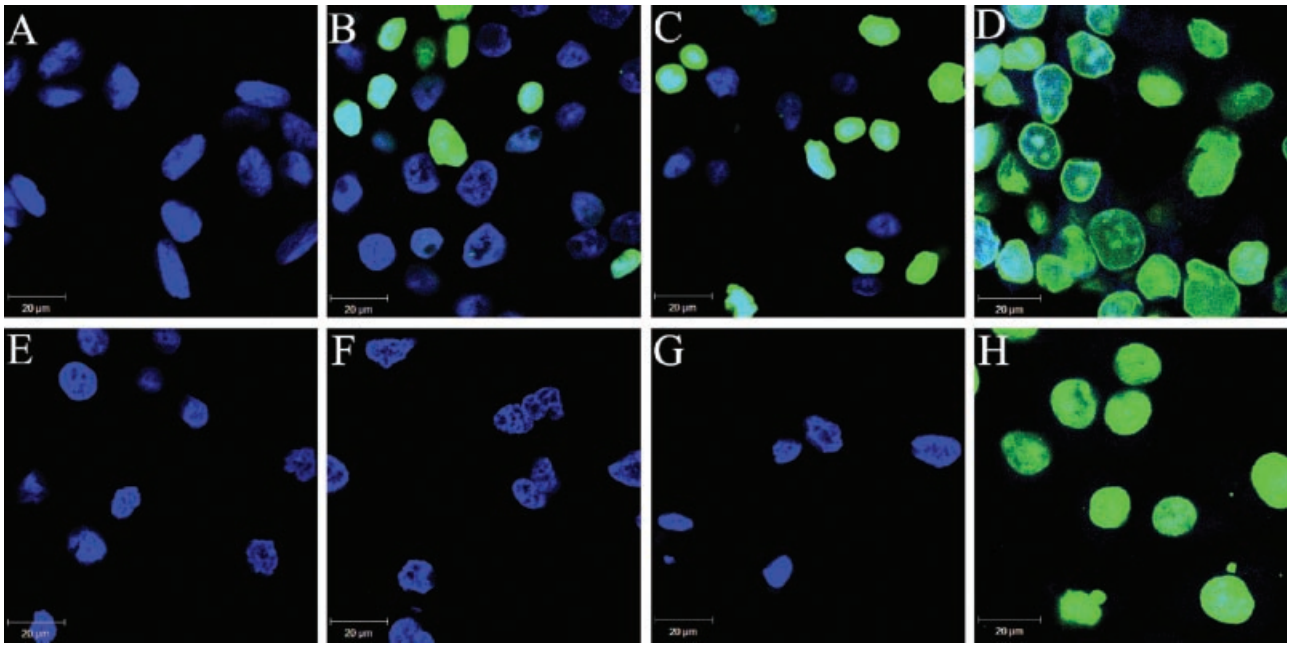

Fig. 2. TUNEL staining of PDT-treated cells. PDT-treated LNCaP cells at 1, 2.5, or 5 μM Ppa-conjugate **2** (**A**–**C**). PDT-treated PC-3 cells at 1, 2.5, or 5 μM Ppa-conjugate **2** (**E**–**G**). PDT-treated LNCaP and PC-3 cells with 2.5 μM free Ppa (**D**,**H**), as control. Cellular nuclei were counterstained by DAPI. Bar scale is 20 μm.

LNCaP cells was observed to be dose-dependent while no effect was observed for PC-3 cells (Fig. 2A–C, E–G). No fluorescent signal from the incorporation of fluorescein-dUTP in LNCaP cells was observed for 1 μM Ppa-conjugate **2** whereas approximately 30% and 60% of the cells gave positive results at 2.5 and 5.0 μM, respectively. In contrast, no detectable incorporation of fluorescein-dUTP was observed at these concentrations in PSMA− cells (PC-3). These latter results revealed the specificity of the Ppa-conjugate **2** toward the PSMA+ LNCaP cells. As an additional control, unconjugated Ppa (2.5 μM) was applied to both LNCaP and PC-3 cells (Fig. 2. D,H). Upon light treatment of these cells, PDT-mediated DNA fragmentation was observed in all cells of both cell lines demonstrating the non-specificity of unconjugated Ppa. These data demonstrate that when coupled, inhibitor core **1** provides Ppa with specificity for PSMA+ cells. This demonstrated specificity addresses the targeting challenge encountered by most conventional PSs.

Dynamics of Cell Membrane Permeability Changes After PDT. Cell membrane permeability of LNCaP cells following PDT treatment with Ppa-conjugate **2** was examined using the differential staining of HOE33342 and PI. HOE33342 is a cell-permeating nuclear counterstain preferentially used with living and unfixed cells, while PI is a membrane-impermeable nucleic acid stain, generally excluded from viable cells. The deployment of both cellular stains can be used to characterize membrane-damage in tumor cells [48]. In negative control experiments, cells were exposed only to light treatment and not pre-incubated with Ppa-conjugate **2**. For these control cells, only HOE33342 was observed to enter and stain the nuclei (Fig. 3A); there was no signal from PI (Fig. 3B). For those cells treated with Ppa-conjugate **2** and then subjected to light treatment, we observed that after 2 hr following light treatment, the nuclei of the cells exhibited greater HOE33342 staining (Fig. 3C) and a weak signal from PI (Fig. 3D). These results suggest that as a result of PDT treatment, the integrity of the cellular membrane was compromised. At 4 hr post-treatment, cells displayed greater membrane damage based on the extent of PI staining (Fig. 3F). This time-dependent of increase in PI staining is indicative of the controlled events associated with apoptosis [48,49]. To confirm that the targeting of Ppa-conjugate **2** for LNCaP cells was due to its interactions with the PSMA biomarker, cells were first treated with the inhibitor core **1** alone prior to administration of Ppa-conjugate 2 (Fig. 3G,H). The lack of PI staining in these cells (Fig. 3H) and nuclear staining by HOE33342 (Fig. 3G) that was similar to the control samples (Fig. 3A). These results suggest that

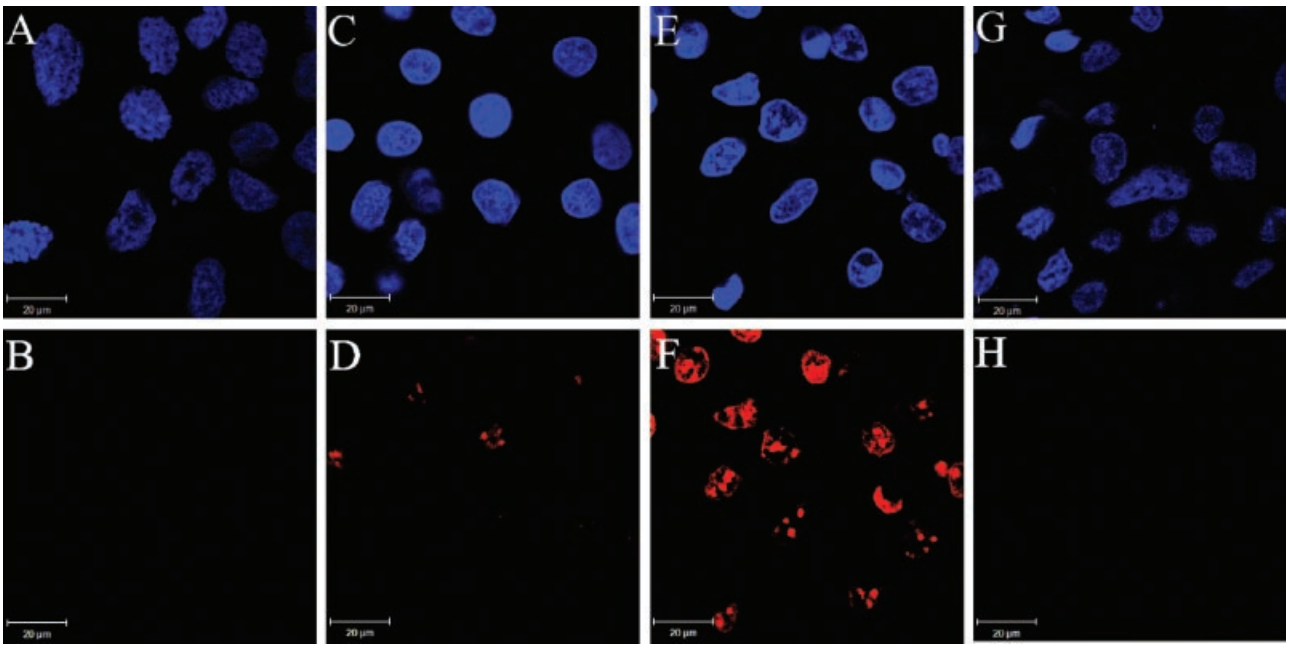

Fig. 3. HOE33342/PI double staining. Post-PDT-treated LNCaP were stained by Hoechst 33342 (**top panels**) and propidium iodide (**bottom panels**) before fixation. Controls **A**,**B**: 4 hr after light exposure; cells were subjected to 10 min light exposure but were not pre-treated with Ppa-conjugate **2**. **C**–**F**: cells were pre-treated with 2.5 μM Ppa-conjugate **2** prior to 10 min light exposure. C,D: 2 hr post-PDT treatment. E,F: 4 hr post-PDT treatment. G,H: 4 hr after light exposure but first pre-treated 30 min with 100 μM inhibitor core **1** prior to pre-treatment with Ppa-conjugate **2**. Double-stained cells were fixed for microscopy visualization. Bar scale is 20 μm.

inhibitor core **1** effectively blocked Ppa-conjugate **2** from binding to the cells thus confirming Ppa-conjugate **2** targets LNCaP cells by binding to PSMA.

PARP Cleavage in PDT-Treated LNCaP Cells. Following PDT treatment of LNCaP cells with Ppa-conjugate **2**, experiments for the cytoimmunofluorescence detection of the p85 cleavage fragment of PARP were performed to provide further evidence of apoptosis through caspace-3/7 activation. The development of fluorescent intensity from the PARP p85 fragment was observed to be time-dependent (Fig. 4E,H). The cytoimmunofluorescence signals of PARP p85 fragment was predominant within nuclei with less being detected in cytoplasmic space (Fig. 4C,F,I) suggesting programmed cell death [50–53]. The time-dependent development of the p85 fragment was correlated with morphological changes in cellular nuclei, which became condensed and spherical by 4 hr post-treatment.

DISCUSSION

In our previous study, we conjugated an amine-reactive fluorescein-based dye to the inhibitor core **1** and demonstrated that this conjugate selectively labeled PSMA+ cells [35]. Furthermore, we confirmed that upon binding to PSMA on these cells, the conjugate was internalized, presumably through the clathrin and filamin associated mechanism responsible for PSMA internalization [54–56]. We observed that the internalization of this fluorescent conjugate was time-dependent, detectable as early as 30 min after incubation with maximum internalization occurring by 150 min at 37°C. As a follow up to this preliminary work, we explored the concept that peptidomimetic PSMA inhibitor **1** could be coupled to a PS for PDT applications in this present study. To this end, the PSMA inhibitor **1** was coupled to the porphyrinic PS Ppa (Fig. 1). The resulting Ppa-conjugate **2** maintained considerable inhibitory potency for PSMA ($IC_{50} = 102$ nM) and

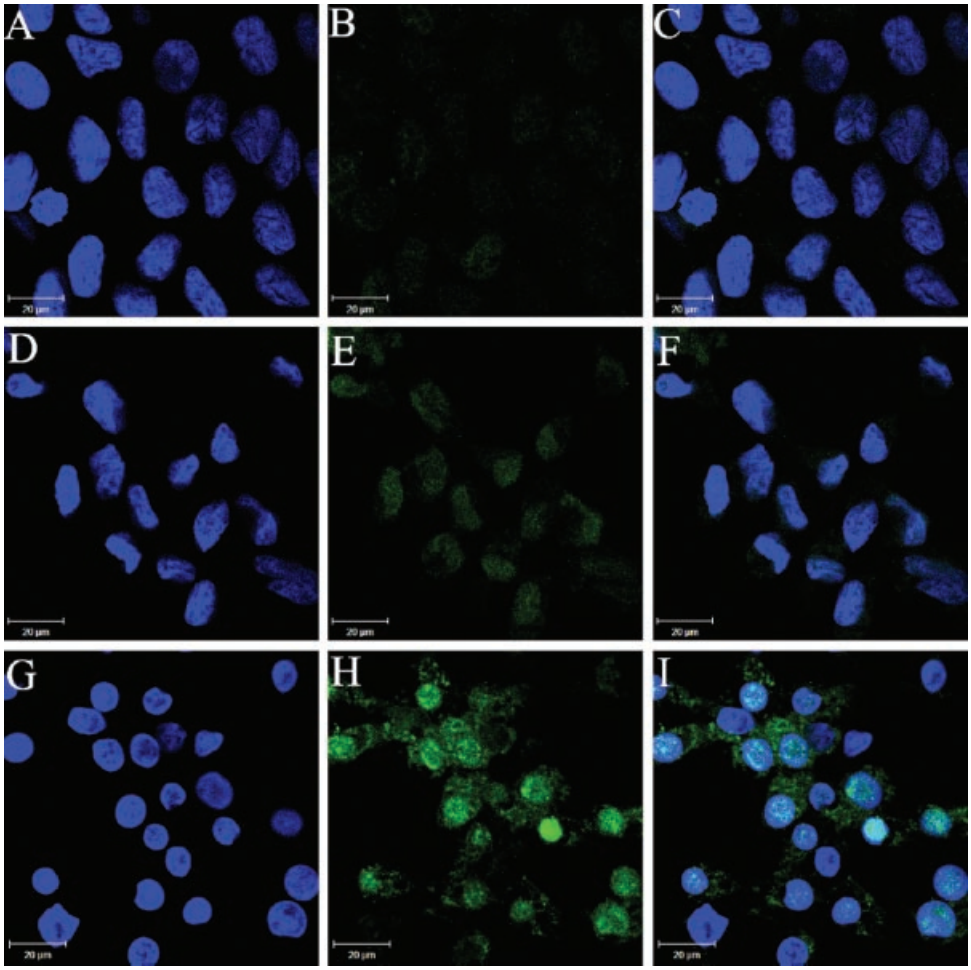

Fig. 4. Cytoimmunofluorescence detection of PARP cleavage p85 fragment following PDT treatment with Ppa-conjugate **2** (2.5 μM). Control cells (light treatment only, no Ppa-conjugate **2** applied (**A**–**C**). Two-hour post-PDT treatment (**D**–**F**). Four-hour post-PDT (**G**–**I**). Cellular nuclei were counterstained by DAPI. A,D,G: DAPI staining. B,E,H: p85 staining. C,F,I: merged DAPI and p85 staining. Bar scale is 20 μm.

demonstrated both selective internalization (Supplementary Material) and targeted PDT capabilities in vitro by selectively inducing apoptosis in PSMA+ prostate cancer cells (LNCaP).

Aromatic PSs are prone to form non-covalent aggregates in aqueous media. As a result, this can lead to diminished singlet oxygen quantum yields and PDT activities. In addition these aggregates are less fluorescent than the corresponding monomers. This problem can be limiting for in vivo PDT applications [57–59]. Furthermore, small lipophilic PS molecules, such as Ppa or its methyl ester, can non-specifically diffuse through cell membranes, and localize in the intracellular membrane system, particularly the endoplasmic reticulum, Golgi apparatus, lysosomes, and mitochondria [36,37]. We hypothesized that coupling inhibitor core **1** to Ppa would simultaneously achieve three goals: promote aqueous solubility of the PS, diminish non-specific diffusion into cells, and specifically target the PS to PSMA+ cells.

In vitro PDT treatment of PSMA+ cells using the Ppa-conjugate **2** resulted in detectable dose-dependent DNA fragmentation 16 hr post-treatment as determined by TUNEL assay. Under the same conditions, a negligible effect was observed at earlier time points (2, 4, and 8 hr, data not shown) consistent with the time-dependent process such as apoptosis. While PSMA+ cells were sensitive to PDT treatment using Ppa-conjugate **2** (2.5 and 5 μM), PSMA− cells (PC-3) were unaffected, thus confirming the specificity of the Ppa-conjugate **2** for PSMA+ cells. In addition, PDT treatment of both LNCaP and PC-3 cells by unconjugated Ppa at 2.5 μM resulted in DNA fragmentation detectable in all cells from both cell lines, thus confirming Ppa's inherent lack of specificity common to simple porphyrinic PSs.

Following PDT treatment of LNCaP cells with Ppa-conjugate **2** (2.5 μM), cell membranes became detectably more permeable by PI staining prior to fixation. The extent of PI staining was time-dependent being observable as early as 2 hr post-treatment. In addition, PARP cleavage was observed by 2 hr following PDT treatment under the same conditions. The detected PARP p85 fragment was predominantly localized within nuclei with less being found in the cytoplasmic space. The time-dependence of p85 fragment formation and membrane permeability was concomitant with morphological changes of cellular nuclei, which became condensed by 4 hr post-treatment. In summary, the data from the in vitro PDT experiments are consistent with an apoptotic mechanism being activated following PDT treatment with Ppa-conjugate **2** [43,44,50–53].

Based on the data from the in vitro PDT experiments, a likely sequence of events triggering apoptosis is as follows: internalization of Ppa-conjugate **2** to endosomes or lysomes, production of singlet oxygen and reactive oxygen species (ROS) upon irradiation, damage to endosomal or lysomal membranes with concomitant release of proteinases activating a caspase cascade pathway toward apoptosis [60,61]. Evidence of PARP cleavage to the p85 fragment is a strong indicator that pro-caspase-3 or 7 were activated through an apoptotic cascade [45,62].

The observation that cells were stained by PI shortly after PDT treatment is consistent with that observed with atypical apoptotic cells [49]. The detection of PARP cleavage and DNA fragmentation in our experiments indicate that the initiation of apoptosis occurred in PDT-treated LNCaP cells with Ppa-conjugate **2**. However, two other downstream hallmarks of apoptosis: phosphatidylserine externalization and DNA ladder formation were not observed (data not shown) [63–66]. Therefore, our findings suggest that the initiated apoptotic sequence did not yet proceed to late-stage apoptosis as a result of plasma membrane damage. Similar observations have been reported in which membrane photodamage has delayed or prevented the apoptotic process [49,67].

Despite being non-specific, Ppa itself is considerably more phototoxic ($LC_{90} = 150$ nM) than the Ppa-conjugate **2** [36]. Presumably, this difference is the result of their differential subcellular localization. Based on our previous studies with a fluorescein-based analog, the Ppa-conjugate **2** is presumably internalized upon binding to extracellular PSMA and is initially restricted to endosomes via PSMA-mediated endocytosis [35]. The mitochondrion has been proposed to be a more critical target organelle to effectively induce apoptosis following PSs-mediated PDT [36]. As such, our future efforts will be aimed at incorporating motifs that facilitate PS escape from endosomal or lysosomal restriction.

In conclusion, we have demonstrated for the first time that small molecule inhibitors of PSMA when conjugated with a PS, are capable of initiating apoptosis upon light treatment. As expected, coupling the inhibitor core **1** to Ppa diminished non-specific diffusion into cells, and specifically targeted the PS to PSMA+ cells. This proof-of concept work now serves as the basis for further development of PDT for prostate cancer and an alternative to antibody-based approaches.

ACKNOWLEDGMENTS

This work was supported in part by the National Institutes of Health (7R21CA122126-03). The authors extend their gratitude for technical assistance to G. Helms and W. Hiscox at the WSU Center for NMR

Spectroscopy and C. Davitt at the WSU Franceschi Microscopy and Imaging Center. The authors also thank M. Holroyd for editorial assistance.

REFERENCES

1. Kessel D. Photodynamic therapy: From the beginning. Photodiagnosis Photodynamic Ther 2004;1(1):3–7.
2. Moan J, Peng Q. An outline of the hundred-year history of PDT. Anticancer Res 2003;23(5A):3591–3600.
3. Ackroyd R, Kelty C, Brown N, Reed M. The history of photodetection and photodynamic therapy. Photochem Photobiol 2001;74(5):656–669.
4. Detty MR, Gibson SL, Wagner SJ. Current clinical and preclinical photosensitizers for use in photodynamic therapy. J Med Chem 2004;47(16):3897–3915.
5. Allison RR, Downie GH, Cuenca R, Hu XH, Childs CJ, Sibata CH. Photosensitizers in clinical PDT. Photodiagnosis Photodynamic Ther 2004;1(1):27–42.
6. Nyman ES, Hynninen PH. Research advances in the use of tetrapyrrolic photosensitizers for photodynamic therapy. J Photochem Photobiol B Biol 2004;73(1):1–28.
7. Berg K, Selbo PK, Weyergang A, Dietze A, Prasmickaite L, Bonsted A, Engesaeter BO, Angell-Petersen E, Warloe T, Frandsen N, Hogset A. Porphyrin-related photosensitizers for cancer imaging and therapeutic applications. J Microsc 2005; 218(Pt 2):133–147.
8. Sharman WM, van Lier JE, Allen CM. Targeted photodynamic therapy via receptor mediated delivery systems. Adv Drug Deliv Rev 2004;56(1):53–76.
9. Stefflova K, Chen J, Zheng G. Killer beacons for combined cancer imaging and therapy. Curr Med Chem 2007;14(20):2110–2125.
10. Johansson A, Axelsson J, Andersson-Engels S, Swartling J. Realtime light dosimetry software tools for interstitial photodynamic therapy of the human prostate. Med Phys 2007; 34(11):4309–4321.
11. Fair WR, Israeli RS, Heston WD. Prostate-specific membrane antigen. Prostate 1997;32(2):140–148.
12. Slovin SF. Targeting novel antigens for prostate cancer treatment: Focus on prostate-specific membrane antigen. Expert Opin Ther Targets 2005;9(3):561–570.
13. Chang SS, O'Keefe DS, Bacich DJ, Reuter VE, Heston WD, Gaudin PB. Prostate-specific membrane antigen is produced in tumor-associated neovasculature. Clin Cancer Res 1999;5(10): 2674–2681.
14. Chang SS, Reuter VE, Heston WD, Gaudin PB. Department of Urologic Surgery VUMCNTUSA. Comparison of anti-prostate-specific membrane antigen antibodies and other immunomarkers in metastatic prostate carcinoma. Urology 2001;57(6):1179–1183.
15. Rosenthal SA, Haseman MK, Polascik TJ, Division of Radiation Oncology RAoSMGICUSA. Utility of capromab pendetide (ProstaScint) imaging in the management of prostate cancer. Tech Urol 2001;7(1):27–37.
16. Bander NH, Milowsky MI, Nanus DM, Kostakoglu L, Vallabhajosula S, Goldsmith SJ. Phase I trial of 177lutetium-labeled J591, a monoclonal antibody to prostate-specific membrane antigen, in patients with androgen-independent prostate cancer. J Clin Oncol 2005;23(21):4591–4601.
17. Chu TC, Shieh F, Lavery LA, Levy M, Richards-Kortum R, Korgel BA, Ellington AD. Labeling tumor cells with fluorescent nanocrystal-aptamer bioconjugates. Biosens Bioelectron 2006; 21(10):1859–1866.
18. Farokhzad OC, Khademhosseini A, Jon S, Hermmann A, Cheng J, Chin C, Kiselyuk A, Teply B, Eng G, Langer R. Microfluidic system for studying the interaction of nanoparticles and microparticles with cells. Anal Chem 2005;77(17):5453–5459.
19. Foss CA, Mease RC, Fan H, Wang Y, Ravert HT, Dannals RF, Olszewski RT, Heston WD, Kozikowski AP, Pomper MG. Radiolabeled small-molecule ligands for prostate-specific membrane antigen: In vivo imaging in experimental models of prostate cancer. Clin Cancer Res 2005;11(11):4022–4028.
20. Gao X, Cui Y, Levenson RM, Chung LW, Nie S. In vivo cancer targeting and imaging with semiconductor quantum dots. Nat Biotechnol 2004;22(8):969–976.
21. Guilarte TR, McGlothan JL, Foss CA, Zhou J, Heston WD, Kozikowski AP, Pomper MG, Department of Environmental Health Sciences JHSoPHBMDUSA. Glutamate carboxypeptidase II levels in rodent brain using [125I]DCIT quantitative autoradiography. Neurosci Lett 2005;387(3):141–144.
22. Humblet V, Lapidus R, Williams LR, Tsukamoto T, Rojas C, Majer P, Hin B, Ohnishi S, De Grand AM, Zaheer A, Renze JT, Nakayama A, Slusher BS, Frangioni JV. High-affinity near-infrared fluorescent small-molecule contrast agents for in vivo imaging of prostate-specific membrane antigen. Mol Imaging 2005;4(4):448–462.
23. Milowsky MI, Nanus DM, Kostakoglu L, Sheehan CE, Vallabhajosula S, Goldsmith SJ, Ross JS, Bander NH. Vascular targeted therapy with anti-prostate-specific membrane antigen monoclonal antibody J591 in advanced solid tumors. J Clin Oncol 2007;25(5):540–547.
24. Pomper MG, Musachio JL, Zhang J, Scheffel U, Zhou Y, Hilton J, Maini A, Dannals RF, Wong DF, Kozikowski AP. 11C-MCG: Synthesis, uptake selectivity, and primate PET of a probe for glutamate carboxypeptidase II (NAALADase). Mol Imaging 2002;1(2):96–101.
25. Smith MR, Nelson JB. Future therapies in hormone-refractory prostate cancer. Urology 2005;65(5 Suppl):9–16, discussion 17.
26. Smith-Jones PM, Vallabhajosula S, Navarro V, Bastidas D, Goldsmith SJ, Bander NH. Radiolabeled monoclonal antibodies specific to the extracellular domain of prostate-specific membrane antigen: Preclinical studies in nude mice bearing LNCaP human prostate tumor. J Nucl Med 2003;44(4):610–617.
27. Tsukamoto T, Wozniak KM, Slusher BS. Progress in the discovery and development of glutamate carboxypeptidase II inhibitors. Drug Discov Today 2007;12(17–18):767–776.
28. Chandran SS, Banerjee SR, Mease RC, Pomper MG, Denmeade SR. Characterization of a targeted nanoparticle functionalized with a urea-based inhibitor of prostate-specific membrane antigen (PSMA). Cancer Biol Ther 2008;7(6):974–982.
29. Banerjee SR, Foss CA, Castanares M, Mease RC, Byun Y, Fox JJ, Hilton J, Lupold SE, Kozikowski AP, Pomper MG. Synthesis and evaluation of technetium-99m- and rhenium-labeled inhibitors of the prostate-specific membrane antigen (PSMA). J Med Chem 2008;51(15):4504–4517.
30. Mease RC, Dusich CL, Foss CA, Ravert HT, Dannals RF, Seidel J, Prideaux A, Fox JJ, Sgouros G, Kozikowski AP, Pomper MG. N-[N-[(S)-1,3-Dicarboxypropyl]carbamoyl]-4-[18F]fluorobenzyl-L-cysteine, [18F]DCFBC: A new imaging probe for prostate cancer. Clin Cancer Res 2008;14(10):3036–3043.
31. Tasch J, Gong M, Sadelain M, Heston WD, Department of Urology MHMS-KCCNYNYUSA. A unique folate hydrolase, prostate-specific membrane antigen (PSMA): A target for immunotherapy? Crit Rev Immunol 2001;21:1–3.

32. Salit RB, Kast WM, Velders MP. Ins and outs of clinical trials with peptide-based vaccines. Front Biosci 2002;7:e204–e213.
33. Lu J, Celis E. Recognition of prostate tumor cells by cytotoxic T lymphocytes specific for prostate-specific membrane antigen. Cancer Res 2002;62(20):5807–5812.
34. Fracasso G, Bellisola G, Cingarlini S, Castelletti D, Prayer-Galetti T, Pagano F, Tridente G, Colombatti M. Anti-tumor effects of toxins targeted to the prostate specific membrane antigen. Prostate 2002;53(1):9–23.
35. Liu T, Wu LY, Kazak M, Berkman CE. Cell-Surface labeling and internalization by a fluorescent inhibitor of prostate-specific membrane antigen. Prostate 2008;68(9):955–964.
36. Savellano MD, Pogue BW, Hoopes PJ, Vitetta ES, Paulsen KD. Multiepitope HER2 targeting enhances photoimmunotherapy of HER2-overexpressing cancer cells with pyropheophorbide-a immunoconjugates. Cancer Res 2005;65(14):6371–6379.
37. Sun X, Leung WN. Photodynamic therapy with pyropheophorbide-a methyl ester in human lung carcinoma cancer cell: Efficacy, localization and apoptosis. Photochem Photobiol 2002;75(6):644–651.
38. Stefflova K, Li H, Chen J, Zheng G. Peptide-based pharmacomodulation of a cancer-targeted optical imaging and photodynamic therapy agent. Bioconjug Chem 2007;18(2):379–388.
39. Wu LY, Anderson MO, Toriyabe Y, Maung J, Campbell TY, Tajon C, Kazak M, Moser J, Berkman CE. The molecular pruning of a phosphoramidate peptidomimetic inhibitor of prostate-specific membrane antigen. Bioorg Med Chem 2007;15(23):7434–7443.
40. Anderson MO, Wu LY, Santiago NM, Moser JM, Rowley JA, Bolstad ES, Berkman CE. Substrate specificity of prostate-specific membrane antigen. Bioorg Med Chem 2007;15(21):6678–6686.
41. Maung J, Mallari JP, Girtsman TA, Wu LY, Rowley JA, Santiago NM, Brunelle AN, Berkman CE. Probing for a hydrophobic a binding register in prostate-specific membrane antigen with phenylalkylphosphonamidates. Bioorg Med Chem 2004;12(18):4969–4979.
42. Liu T, Toriyabe Y, Berkman CE. Purification of prostate-specific membrane antigen using conformational epitope-specific antibody-affinity chromatography. Protein Expr Purif 2006;49(2):251–255.
43. Willingham MC. Cytochemical methods for the detection of apoptosis. J Histochem Cytochem 1999;47(9):1101–1110.
44. Allen RT, Hunter WJ III, Agrawal DK. Morphological and biochemical characterization and analysis of apoptosis. J Pharmacol Toxicol Methods 1997;37(4):215–228.
45. Matroule JY, Carthy CM, Granville DJ, Jolois O, Hunt DW, Piette J. Mechanism of colon cancer cell apoptosis mediated by pyropheophorbide-a methylester photosensitization. Oncogene 2001;20(30):4070–4084.
46. Inoue H, Kajimoto Y, Shibata MA, Miyoshi N, Ogawa N, Miyatake S, Otsuki Y, Kuroiwa T. Massive apoptotic cell death of human glioma cells via a mitochondrial pathway following 5-aminolevulinic acid-mediated photodynamic therapy. J Neurooncol 2007;83(3):223–231.
47. Yslas EI, Durantini EN, Rivarola VA. Zinc-(II) 2,9,16,23-tetrakis (methoxy) phthalocyanine: Potential photosensitizer for use in photodynamic therapy in vitro. Bioorg Med Chem 2007;15(13):4651–4660.
48. Sharma S, Dube A, Bose B, Gupta PK. Pharmacokinetics and phototoxicity of purpurin-18 in human colon carcinoma cells using liposomes as delivery vehicles. Cancer Chemother Pharmacol 2006;57(4):500–506.
49. Hsieh YJ, Wu CC, Chang CJ, Yu JS. Subcellular localization of Photofrin determines the death phenotype of human epidermoid carcinoma A431 cells triggered by photodynamic therapy: When plasma membranes are the main targets. J Cell Physiol 2003;194(3):363–375.
50. Alvarez-Gonzalez R, Spring H, Muller M, Burkle A. Selective loss of poly(ADP-ribose) and the 85-kDa fragment of poly-(ADP-ribose) polymerase in nucleoli during alkylation-induced apoptosis of HeLa cells. J Biol Chem 1999;274(45):32122–32126.
51. Li X, Darzynkiewicz Z. Cleavage of Poly(ADP-ribose) polymerase measured in situ in individual cells: Relationship to DNA fragmentation and cell cycle position during apoptosis. Exp Cell Res 2000;255(1):125–132.
52. He J, Whitacre CM, Xue LY, Berger NA, Oleinick NL. Protease activation and cleavage of poly(ADP-ribose) polymerase: An integral part of apoptosis in response to photodynamic treatment. Cancer Res 1998;58(5):940–946.
53. Kaufmann SH, Desnoyers S, Ottaviano Y, Davidson NE, Poirier GG. Specific proteolytic cleavage of poly(ADP-ribose) polymerase: An early marker of chemotherapy-induced apoptosis. Cancer Res 1993;53(17):3976–3985.
54. Anilkumar G, Rajasekaran SA, Wang S, Hankinson O, Bander NH, Rajasekaran AK. Prostate-specific membrane antigen association with filamin A modulates its internalization and NAALADase activity. Cancer Res 2003;63(10):2645–2648.
55. Liu H, Rajasekaran AK, Moy P, Xia Y, Kim S, Navarro V, Rahmati R, Bander NH. Constitutive and antibody-induced internalization of prostate-specific membrane antigen. Cancer Res 1998;58(18):4055–4060.
56. Rajasekaran SA, Anilkumar G, Oshima E, Bowie JU, Liu H, Heston W, Bander NH, Rajasekaran AK. A novel cytoplasmic tail MXXXL motif mediates the internalization of prostate-specific membrane antigen. Mol Biol Cell 2003;14(12):4835–4845.
57. Bonnett R, Martinez G. Photobleaching of compounds of the 5,10,15,20-Tetrakis(m-hydroxyphenyl)porphyrin Series (m-THPP, m-THPC, and m-THPBC). Org Lett 2002;4(12):2013–2016.
58. Strauss WS, Sailer R, Gschwend MH, Emmert H, Steiner R, Schneckenburger H. Selective examination of plasma membrane-associated photosensitizers using total internal reflection fluorescence spectroscopy: Correlation between photobleaching and photodynamic efficacy of protoporphyrin IX. Photochem Photobiol 1998;67(3):363–369.
59. Brasseur N, Ouellet R, La Madeleine C, van Lier JE. Water-soluble aluminium phthalocyanine-polymer conjugates for PDT: Photodynamic activities and pharmacokinetics in tumour-bearing mice. Br J Cancer 1999;80(10):1533–1541.
60. Caruso JA, Mathieu PA, Reiners JJ Jr. Sphingomyelins suppress the targeted disruption of lysosomes/endosomes by the photosensitizer NPe6 during photodynamic therapy. Biochem J 2005;392(Pt 2):325–334.
61. Brunk UT, Dalen H, Roberg K, Hellquist HB. Photo-oxidative disruption of lysosomal membranes causes apoptosis of cultured human fibroblasts. Free Radic Biol Med 1997;23(4):616–626.
62. Buytaert E, Dewaele M, Agostinis P. Molecular effectors of multiple cell death pathways initiated by photodynamic therapy. Biochim Biophys Acta 2007;1776(1):86–107.
63. Liu X, Zou H, Slaughter C, Wang X, DFF, a heterodimeric protein that functions downstream of caspase-3 to trigger DNA fragmentation during apoptosis. Cell 1997;89(2):175–184.

64. Naito M, Nagashima K, Mashima T, Tsuruo T. Phosphatidylserine externalization is a downstream event of interleukin-1 beta-converting enzyme family protease activation during apoptosis. Blood 1997;89(6):2060–2066.
65. Enari M, Sakahira H, Yokoyama H, Okawa K, Iwamatsu A, Nagata S. A caspase-activated DNase that degrades DNA during apoptosis, and its inhibitor ICAD. Nature 1998;391(6662):43–50.
66. Yu A, Byers DM, Ridgway ND, McMaster CR, Cook HW. Preferential externalization of newly synthesized phosphatidylserine in apoptotic U937 cells is dependent on caspase-mediated pathways. Biochim Biophys Acta 2000;1487(2–3):296–308.
67. Kessel D, Luo Y, Deng Y, Chang CK. The role of subcellular localization in initiation of apoptosis by photodynamic therapy. Photochem Photobiol 1997;65(3):422–426.